Mechanics Research Communications 56 (2014) 18–25

Contents lists available at ScienceDirect

Mechanics Research Communications

journal homepage: www.elsevier.com/locate/mechrescom

A discrete-to-continuum approach to the curvatures of membrane networks and parametric surfaces

F. Fraternali[a,*], I. Farina[b], G. Carpentieri[a]

[a] Department of Civil Engineering, University of Salerno, 84084 Fisciano, SA, Italy
[b] Department of Materials Science and Engineering, University of Sheffield, Mappin Street, Sheffield S1 3JD, UK

ARTICLE INFO

Article history:
Received 20 June 2013
Received in revised form 15 October 2013
Accepted 21 October 2013
Available online 6 November 2013

Keywords:
Membrane networks
Multiscale approaches
Bending energy
Parametric surfaces
Mean curvature
Gaussian curvature

ABSTRACT

The present work deals with a scale bridging approach to the curvatures of discrete models of structural membranes, to be employed for an effective characterization of the bending energy of flexible membranes, and the optimal design of parametric surfaces and vaulted structures. We fit a smooth surface model to the data set associated with the vertices of a patch of an unstructured polyhedral surface. Next, we project the fitting function over a structured lattice, obtaining a 'regularized' polyhedral surface. The latter is employed to define suitable discrete notions of the mean and Gaussian curvatures. A numerical convergence study shows that such curvature measures exhibit strong convergence in the continuum limit, when the fitting model consists of polynomials of sufficiently high degree. Comparisons between the present method and alternative approaches available in the literature are given.

© 2013 Elsevier Ltd. All rights reserved.

1. Introduction

The elastic response in bending of structural and biological membrane models is often described through surface energies depending on the curvature tensor of the membrane ('curvature energy', refer, e.g., to Helfrich, 1973; Seung and Nelson, 1988; Helfrich and Kozlov, 1993; Gompper and Kroll, 1996; Discher et al., 1997; Hartmann, 2010; Fraternali and Marcelli, 2012; Schmidt and Fraternali, 2012). One of the most frequently employed bending energy models is the so-called Helfrich energy, which has the following structure

$$E^{bend} = \int_S \left(\frac{\kappa_H}{2} \hat{H}^2 + \kappa_G K \right) dS$$

where S is the current configuration of the membrane; $\hat{H}$ is twice the mean curvature H (i.e., the sum of the two principal curvatures); K is the Gaussian curvature (the product of the two principal curvatures); and κ_H and κ_G are suitable stiffness parameters (Helfrich, 1973; Seung and Nelson, 1988). Once κ_H and κ_G are given, it is clear that the computation of such an energy entirely relies on the estimates of the curvatures H and K. Membrane network models often make use of triangulated membrane networks, and short-range or long-range pair interactions (Seung and Nelson, 1988; Marcelli et al., 2005; Dao et al., 2006; Fraternali and Marcelli, 2012; Schmidt and Fraternali, 2012). A correct estimation of the curvature energy of such models plays a special role when modeling the mechanics of heavily deformed networks (Espriu, 1987; Seung and Nelson, 1988; Bailiie et al., 1990; Gompper and Kroll, 1996). Energy minimization, surface smoothing and curvature estimation of discrete surface models are also challenging problems of computational geometry, and their physical, structural, and architectural implications attract the interest of researchers working in different areas (refer, e.g., to Bartesaghi and Sapiro, 2001; Bechthold, 2004; Pottman et al., 2007; El Sayed et al., 2009; Pottman, 2010; Stratil, 2010; Fraternali, 2010; Datta et al., 2011; Raney et al., 2011; Sullivan, 2008; Wardetzky, 2008). Polyhedral surfaces are frequently employed to discretize parametric surfaces within CAD, CAE and CAM systems (Rypl and Bittnar, 2006), and their regularization at the continuum is important when dealing, e.g., with the parametric design and/or the prototype fabrication of structural surfaces and vaulted structures (Bechthold, 2004; Fu et al., 2008; Pottman et al., 2007; Stratil, 2010; Datta et al., 2011).

The present work deals with a discrete-to-continuum approach to the curvatures of discrete membranes models, which looks at the continuum limits of suitable discrete definitions of such quantities. It is known from the literature that numeric approaches of the curvatures of polyhedral surfaces may feature oscillating behavior in the continuum limit (weak convergence), in presence of arbitrary

* Corresponding author. Tel.: +39 089 964083; fax: +39 089 964045.
E-mail addresses: f.fraternali@unisa.it (F. Fraternali), ifarina1@sheffield.ac.uk (I. Farina), gcarpentieri@unisa.it (G. Carpentieri).

0093-6413/$ – see front matter © 2013 Elsevier Ltd. All rights reserved.
http://dx.doi.org/10.1016/j.mechrescom.2013.10.015

tessellation patterns (cf. e.g., the example in Fig. 4 of Wardetzky, 2008). The present approach aims to circumvent such convergence issues, by fitting a smooth surface model to the data set associated with the vertices of a patch of an arbitrary polyhedral surface. We evaluate the fitting function at the nodes of a structured lattice, generating a new polyhedral surface with ordered structure, and 'regularized' discrete definitions of the membrane curvatures. The remainder of the paper is organized as follows. We begin by briefly recalling the mathematical definitions of the curvatures of smooth membranes in Section 2. Next, we formulate the proposed regularization procedure in Section 3. We study the convergence behavior of the given curvature measures with reference to a model problem (Section 4). We draw the main conclusions the present work in Section 5, where we also discuss potential applications and future extensions of the current research.

2. Monge description of a membrane network

Let us consider a given discrete set X_N of N nodes (or particles) extracted from a membrane network, which have Cartesian coordinates $\{x_{a_1}, x_{a_2}, z_a\}$ $(a = 1, \ldots, N)$ with respect to a given frame $\{O, x_1, x_2, z \equiv x_3\}$ (Fig. 1). We introduce a continuum regularization of X_N through the following Monge chart

$$z_N(\mathbf{x}) = \sum_{a=1}^{N} z_a g_a(\mathbf{x}), \tag{1}$$

where g_a are suitable *shape functions*, and $\mathbf{x} = \{x_1, x_2\}$ denotes the position vector in the x_1, x_2 plane.

The Monge map (1) is defined locally when dealing with complex surfaces and/or closed membranes. In such a case, the axes $\{x_1, x_2\}$ are conveniently drawn on a plane perpendicular to a local estimate of the normal to the corresponding surface (refer, e.g., to (Fraternali et al., 2012) for a detailed illustration of such a covering technique). We name 'platform' the orthogonal projection of X_N onto the x_1, x_2 plane, and we look at x_1 and x_2 as *curvilinear coordinates* of the membrane. If the shape functions g_a are sufficiently smooth, it is an easy task to compute the first fundamental forms $a_{\alpha\beta}$ and the second fundamental forms $b_{\alpha\beta}$ of z_N (refer, e.g. to Kühnel, 2002; Fraternali et al., 2012). The unit tangents $\boldsymbol{\nu}_{\langle 1\rangle}$, $\boldsymbol{\nu}_{\langle 2\rangle}$ to the lines of curvature, and the principal curvatures k_1, k_2 are then obtained from the eigenvalue problem

$$(b_{\alpha\beta} - k_\gamma a_{\alpha\beta})\nu^{\beta}_{\langle\gamma\rangle} = 0 \quad (\gamma = 1, 2) \tag{2}$$

3. A bridging scale approach to the curvatures of polyhedral surfaces

In the special case of a polyhedral membrane, the definition of the fundamental forms and principal curvatures relies on a suitable generalized definition of the *hessian* of z_N, i.e., the second order tensor $\mathbf{H}z_N$ with Cartesian components $z_{N,\alpha\beta}$ (we let $z_{N,\alpha}$ denote the partial derivative of z_N with respect to x_α). Indeed, in such a case, the shape function g_a are piecewise linear functions, and the second-order derivatives of the Monge map (1) exist only in the distributional sense (refer, e.g., to Davini and Paroni, 2003; Sullivan, 2008; Wardetzky, 2008). Throughout the rest of the paper, we focus our attention on a triangulated membrane network, letting Π_N indicate the triangulation that is obtained by projecting such a network over the platform Ω. We denote the position vector of the generic node of Π_N by $\mathbf{x}_n$, and the corresponding coordination number by S_n. In addition, we indicate the edges attached to $\mathbf{x}_n$ by $\Gamma_n^1, \ldots, \Gamma_n^{S_n}$; and the unit vectors perpendicular and tangent to such edges by $\mathbf{h}_n^1, \ldots, \mathbf{h}_n^{S_n}$, and $\mathbf{k}_n^1, \ldots, \mathbf{k}_n^{S_n}$, respectively (Fig. 1). Beside Π_N, we introduce a dual mesh of Ω, which is formed by polygons connecting the barycenters of the triangles attached to $\mathbf{x}_n$ to the mid-points of the edges $\Gamma_n^1, \ldots, \Gamma_n^{S_n}$ ('barycentric' dual mesh, cf. Fig. 1). We say that Π_N is a *structured triangulation* of Ω if, given any tensor $\mathbf{H}$ independent of position, it results

$$\sum_{j=1}^{S_n+1} \int_{G_n} \mathbf{H}(\mathbf{x} - \mathbf{x}_n^j)\cdot(\mathbf{x} - \mathbf{x}_n^j)\nabla g_n^j \otimes \nabla g_n = \mathbf{0} \tag{3}$$

in correspondence with each node $\mathbf{x}_n$. Here, $\mathbf{x}_n^1, \ldots, \mathbf{x}_n^{S_n}$ are the nearest neighbors of $\mathbf{x}_n$; $\mathbf{x}_n^{S_n+1} = \mathbf{x}_n$; G_n is the union of the triangles attached to $\mathbf{x}_n$; and g_n^j is the shape function associated with $\mathbf{x}_n^j$ (refer, e.g., to the benchmark examples shown in Fig. 2).

A discrete definition of the hessian of a polyhedral surface z_N is obtained by introducing a piecewise constant tensor field $\mathbf{H}_N z_N$ over the dual mesh $\hat{\Pi}_N$, which takes the following value over the generic dual cell $\hat{\Omega}_n$ (cf. e.g., Fraternali et al., 2002; Fraternali, 2007)

$$\mathbf{H}_N z_N(n) = \frac{1}{|\hat{\Omega}_n|}\sum_{j=1}^{S_n} \frac{\ell_n^j}{2}\left[\left[\frac{\delta z_N}{\delta h}\right]\right]_n^j \mathbf{h}_n^j \otimes \mathbf{h}_n^j \tag{4}$$

Here, $[[\delta z_N/\delta h]]_n^j$ indicates the jump in the directional derivative $\nabla z_N \cdot \mathbf{h}_n^j$ across the edge Γ_n^j, and ℓ_n^j denotes the length of Γ_n^j. It is worth noting that the trace of $\mathbf{H}_N z_N(n)$ provides a discrete definition of the Lapalacian of z_N (refer to Davini and Paroni, 2003; Fraternali, 2007 for further details). We associate the discrete hessian $\mathbf{H}_N z_N(n)$, and the following weighted gradient (Taubin, 1995)

$$\nabla_N z_N(n) = \frac{1}{3|\hat{\Omega}_n|}\sum_{j=1}^{S_n} \nabla z_N^j |T_n^j| \tag{5}$$

to the generic node of Π_N. In (5), ∇z_N^j denotes the gradient of z_N over the jth triangle attached to $\mathbf{x}_n$, and $|T_n^j|$ denotes the area of such a triangle.

Let us consider now families of triangulations Π_N that show increasing numbers of nodes N, and are such that the *mesh size* $h_N = \sup_{\Omega_m \in \Pi_N}\{\mathrm{diam}(\Omega_m)\}$ approaches zero, as N goes to infinity. We associate a polyhedral surface $z_N(\mathbf{x})$ to each of such triangulations, by projecting a given smooth surface map $z_0(\mathbf{x})$ over Π_N. Referring to structured triangulations, it can be proved that the sequence of the discrete hessians $\mathbf{H}_N z_N$ converges to the hessian of z_0, as N goes to infinity (cf. Lemma 2 of Fraternali, 2007). Unfortunately, such a nice convergence property is not guaranteed if the triangulations Π_N do not match the property (3) ('*unstructured triangulations*'). Let K_n denote a 'patch' of an unstructured triangulation Π_N, which is formed by the k nearest neighbors of $\underline{x}_n$, $k \geq 1$ being a given integer. In order to tackle convergence issues, we construct a smooth fitting function $\tilde{f}_n(\mathbf{x})$ of the values taken by z_N at the vertices of K_n. Next, we evaluate $\tilde{f}_n(\mathbf{x})$ at the vertices $\tilde{\mathbf{x}}_1, \ldots, \tilde{\mathbf{x}}_{\tilde{N}}$ of a second, structured triangulation $\tilde{\Pi}_n$ of the platform (or a portion of Ω comprising $\mathbf{x}_n$), and build up the following 'regularized' polyhedral surface

$$\tilde{z}_n = \sum_{m=1}^{\tilde{N}} \tilde{f}_n(\tilde{\mathbf{x}}_m)\tilde{g}_m \tag{6}$$

The fitting model $\tilde{f}_n$ might consist of suitable interpolation polynomials associated with K_n, local maximum entropy shape functions, B-Splines, Non-Uniform Rational B-Splines (NURBS), or other fitting functions available in standard software libraries. In (6), $\tilde{g}_m$ denotes the shape function associated with the current node $\tilde{\mathbf{x}}_m \in \tilde{\Pi}_n$. By replacing z_N with $\tilde{z}_n$ in Eqs. (4) and (5), we finally endow $\mathbf{x}_n$ with a regularized discrete hessian $\mathbf{H}_N \tilde{z}_N(n)$, and a regularized discrete gradient $\nabla_N \tilde{z}_N(n)$. Straightforward manipulations of the

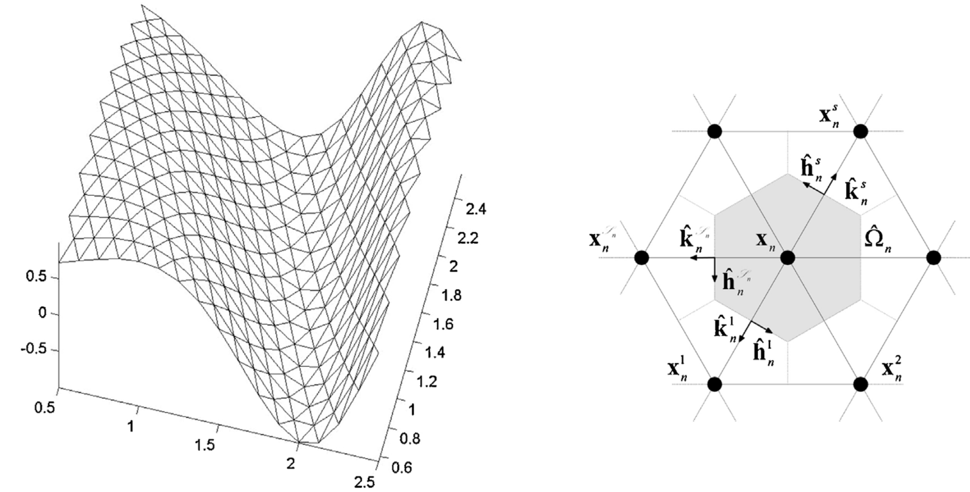

Fig. 1. Illustration of a membrane network (left), and close up of the generic node of a structured triangulation of the platform (right).

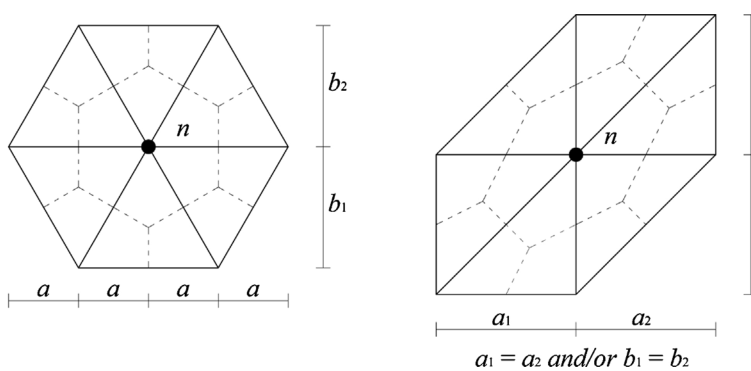

Fig. 2. Patches of triangulations matching property (3).

above gradients and hessians lead us to generalized notions of the fundamental forms and principal curvatures of the discrete surface (cf. Section 2).

4. Numerical results

We test the convergence properties of the regularization technique presented in the previous section by dealing with the mean and Gaussian curvatures of the sinusoidal surface $z_0 = sin(x_1^2 + x_2)$, over the (x_1, x_2) domain $\Omega = [0.5, 2.5] \times [0.5, 2.5]$ (Fig. 1, left). Such a challenging example has already been analyzed in Fraternali et al. (2012), through a different approach based on local maximum entropy shape functions. We analyze four structured triangulations of Ω, which are associated with hexagonal lattices of the platform (cf. Fig. 2, left, with $h = a = b_1 = b_2 = \text{const}$). The analyzed meshes feature 8×8 (mesh $\hat{\Pi}_N^1$); 16×16 (mesh $\hat{\Pi}_N^2$); 32×32 (mesh $\hat{\Pi}_N^3$); and 64×64 (mesh $\hat{\Pi}_N^4$) nodes, respectively. Parallely, we analyze four unstructured triangulations of Ω (meshes $\Pi_N^1, \ldots, \Pi_N^4$), which are obtained through random perturbations of the vertices of $\tilde{\Pi}_N^1, \ldots, \tilde{\Pi}_N^4$ (refer, e.g., to Fig. 3). The pitches h_i of the

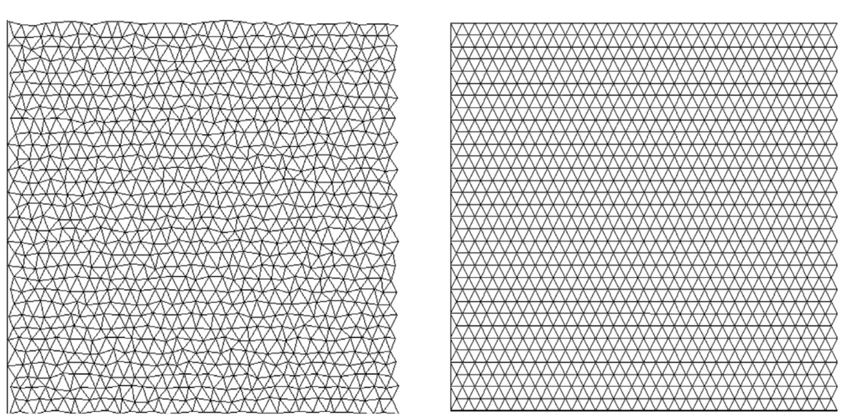

Fig. 3. Illustration of meshes Π_N^3 (left), and $\tilde{\Pi}_N^3$ (right).

Table 1
Root mean square deviations of different approximations to the mean and Gaussian curvatures of the sinusoidal surface $z_0 = sin(x_1^2 + x_2)$.

	Case A		Case B		Case C		e_H^*	e_K^*
	e_H	e_K	e_H	e_K	e_H	e_K		
Mesh 1	0.093	8.925	0.043	9.713	0.031	5.028	0.088	2.733
Relative CPU	1.00		1.46		4.31		1.15	
Mesh 2	0.039	9.344	0.019	4.778	0.009	2.067	0.071	4.597
Relative CPU	1.00		1.49		9.90		1.13	
Mesh 3	0.024	8.672	0.019	7.826	0.003	0.784	0.062	4.015
Relative CPU	1.00		1.26		42.15		1.03	
Mesh 4	0.015	9.536	0.018	7.335	0.001	0.344	0.053	5.004
Relative CPU	1.00		1.25		210.94		1.08	

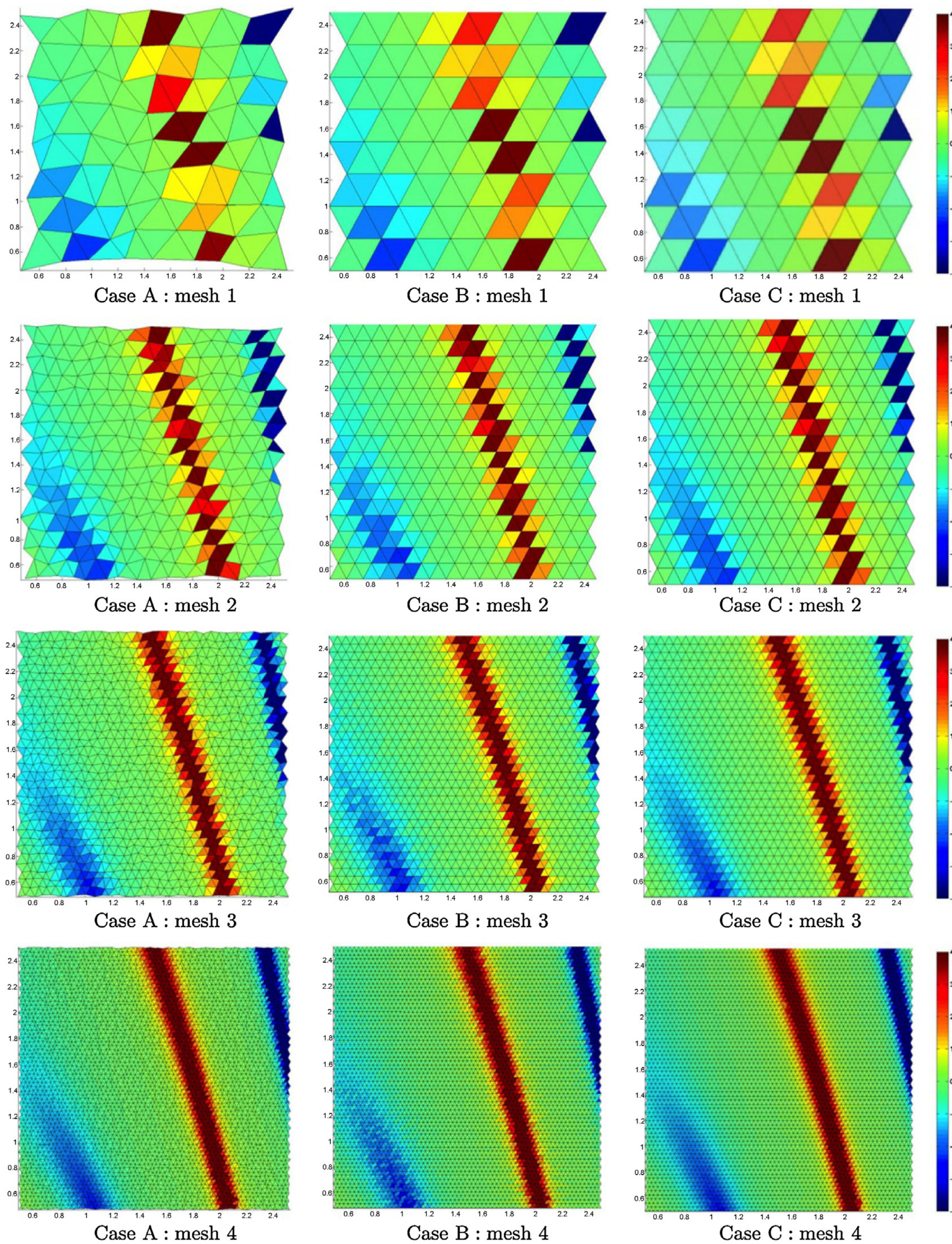

Fig. 4. Density plots of the current approximations to the mean curvature H_0 of the sinusoidal surface $z_0 = sin(x_1^2 + x_2)$ over the x_1, x_2 domain $[0.5, 2.5] \times [0.5, 2.5]$, for different meshes and approximation schemes.

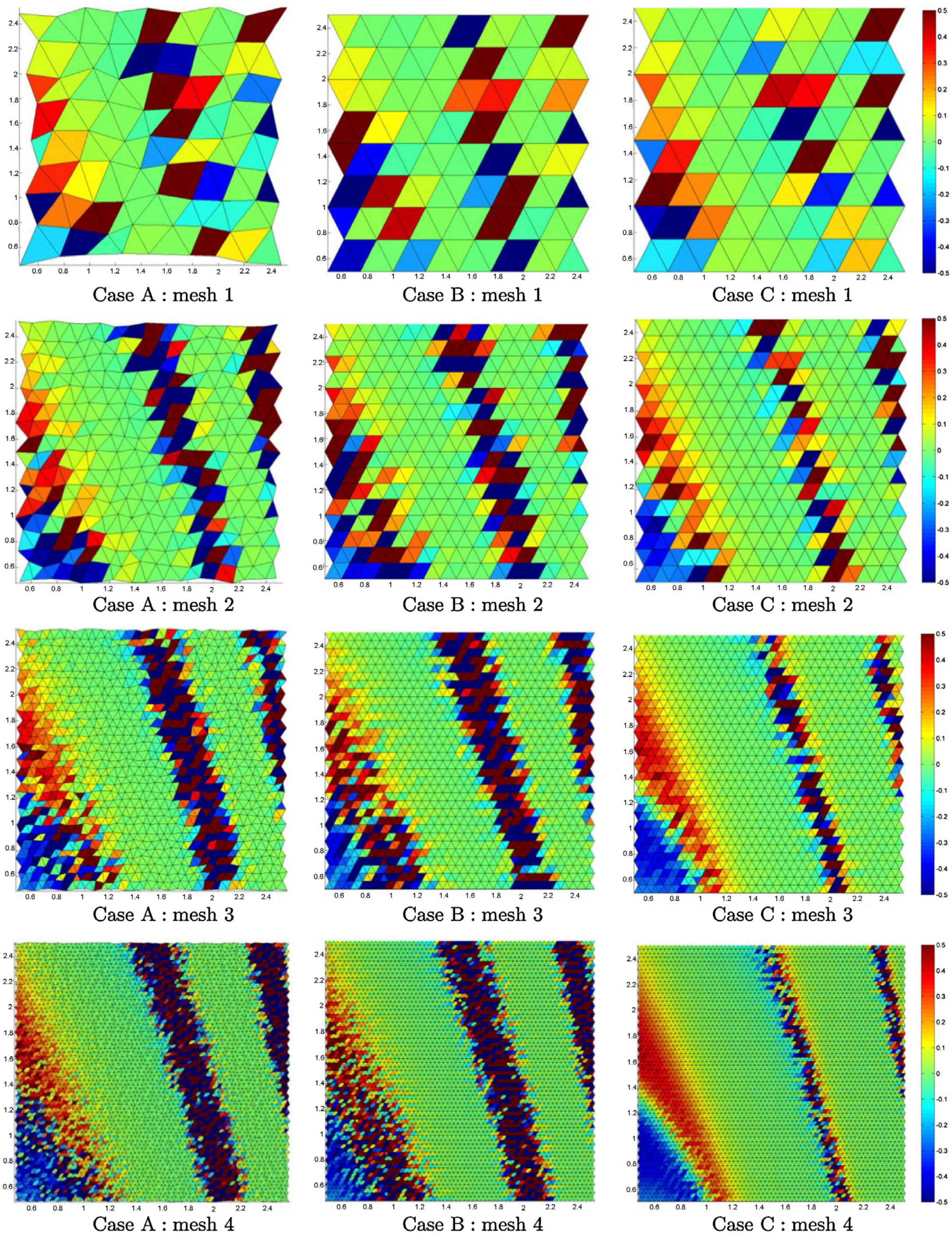

Fig. 5. Density plots of the current approximations to the Gaussian curvature K_0 of the sinusoidal surface $z_0 = sin(x_1^2 + x_2)$ over the x_1, x_2 domain [0.5, 2.5] × [0.5, 2.5], for different meshes and approximation schemes.

meshes $\tilde{\Pi}_N^i$ are such that it results: $h_1 = 0.25$; $h_2 = h_1/2 = 0.125$; $h_3 = h_2/2 = 0.0625$; $h_4 = h_3/2 = 0.03125$. We name 'case A' the approximation method based on polyhedral projections $z_N^1, \ldots, z_N^4$ of z_0 over the unstructured meshes $\Pi_N^1, \ldots, \Pi_N^4$, respectively. We instead name 'case B' the approximation method based on the linear interpolation of $z_N^1, \ldots, z_N^4$ at the vertices of the structured triangulations $\tilde{\Pi}_N^1, \ldots, \tilde{\Pi}_N^4$. Finally, we name 'case C' the approximation scheme based on smooth regularizations $\tilde{z}_N^1, \ldots, \tilde{z}_N^4$ of $z_N^1, \ldots, z_N^4$ over the structured meshes $\tilde{\Pi}_N^1, \ldots, \tilde{\Pi}_N^4$, respectively. The generic of such $\tilde{z}_N^i$ is obtained via the method of local quintic polynomial interpolation and smooth surface fitting presented in Akima and Ortiz (1978), by letting the fitting patch K_n coincide with the entire Π_N^i, in correspondence with each node $\mathbf{x}_n$ (cf. Section 3). We compare the predictions of the above approximation schemes with two alternative discrete predictions H_N^* and K_N^* of the curvatures of the unstructured surfaces $z_N^i (i = 1, \ldots, 4)$. The mean curvature H_N^* is computed as the ratio of the modulus of the area gradient and the modulus of the volume gradient, while the Gaussian curvature K_N^* is computed through the so-called 'angle deficit' formula (refer, e.g., to Sullivan, 2008; Wardetzky, 2008; Fu et al., 2008 for the details of such

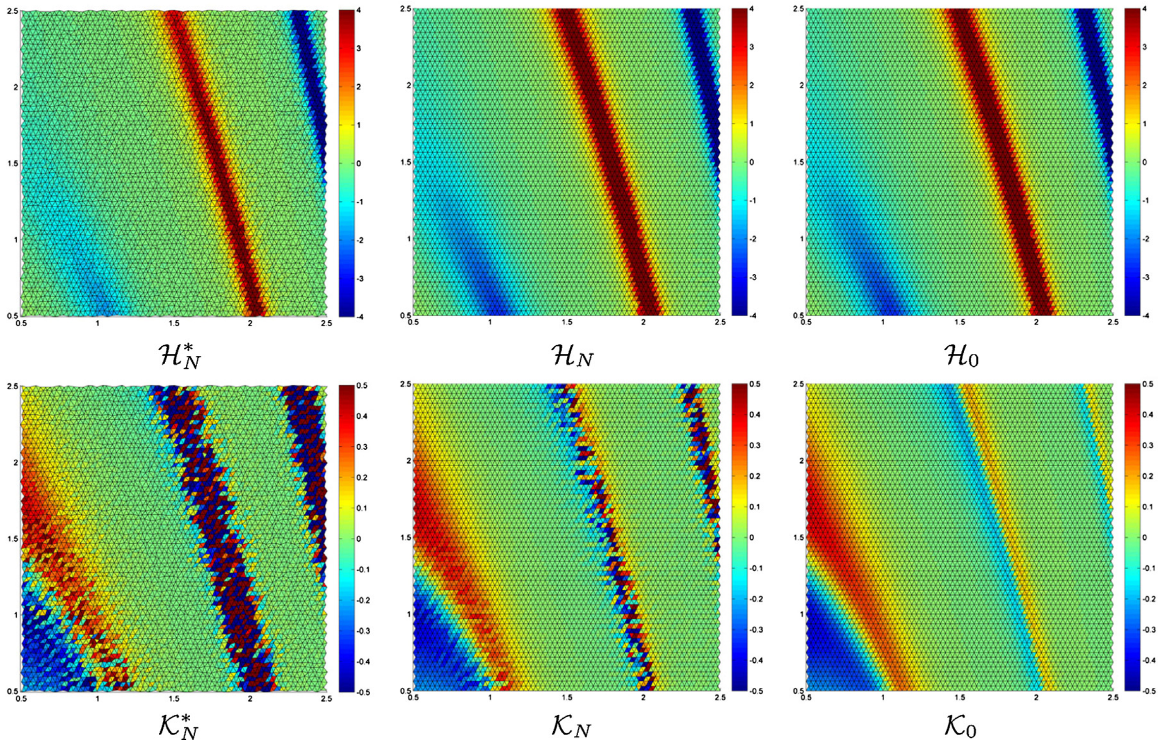

Fig. 6. Comparisons between the approximations H_N and K_N corresponding to case C; the comparative approximations H_N^* and K_N^*; and the exact distributions H_0 and K_0 (mesh 4).

methods). All the above predictions are computed through Matlab® codes.

We measure the accuracy of the analyzed approximation schemes through the following root mean square errors

$$\mathrm{err}_H = \sqrt{\left(\sum_{a=1}^{N}(H_N^a - H_0^a)^2\right)/N}, \ \mathrm{err}_K = \sqrt{\left(\sum_{a=1}^{N}(K_N^a - K_0^a)^2\right)/N} \quad (7)$$

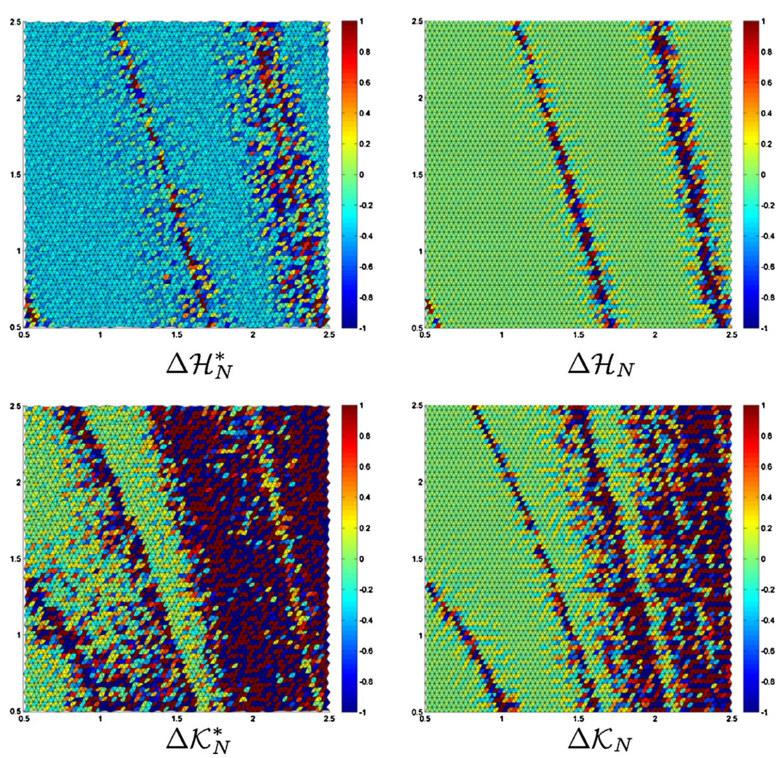

Fig. 7. Density plots of the approximations errors ΔH_N and ΔK_N corresponding to case C, and the comparative errors ΔH_N^* and ΔK_N^* (mesh 4).

where H_N^a and K_N^a denote the values at node a of the current approximation to the mean and Gaussian curvatures, respectively, while H_0^a and K_0^a denote the exact values of the same quantities. The latter can be easily computed through exact differentiation of the surface map z_0 (cf. Section 2), obtaining

$$H_0 = \frac{-(4x_1^2+1)\sin(x_1^2+x_2)+2\cos^3(x_1^2+x_2)+2\cos(x_1^2+x_2)}{2((4x_1^2+1)\cos^2(x_1^2+x_2)+1)^{3/2}} \quad (8)$$

$$K_0 = -\frac{\sin(2(x_1^2+x_2))}{((4x_1^2+1)\cos^2(x_1^2+x_2)+1)^2} \quad (9)$$

Table 1 illustrates the results of the present convergence study in terms of the dimensionless quantities $e_H = \text{err}_H/H_{\max}$ and $e_K = \text{err}_K/K_{\max}$, where $H_{\max}$ and $K_{\max}$ denote the maximum absolute values of the exact mean and Gaussian curvatures over Ω, respectively ($H_{\max} \approx 13.0$; $K_{\max} \approx 0.42$). The same table also provides the approximation errors e_H^* and e_K^* of the predictions H_N^* and K_N^*, and the relative CPU times required to complete the examined simulations (elapsed CPU time required to complete the current example divided by the CPU time required to complete case A, for the same mesh size). Density plots of the current approximations to H_0 and K_0 are presented in Figs. 4–6. Fig. 7 provides additional density plots of the local approximations errors $\Delta H_N = (H_N - H_0)/H_0$ and $\Delta K_N = (K_N - K_0)/K_0$ relative to case C and mesh $\tilde{\Pi}_4$, and the local errors $\Delta H_N^* = (H_N^* - H_0)/H_0$ and $\Delta K_N^* = (K_N^* - K_0)/K_0$ for mesh Π_4. The results in Table 1 highlight that the approximation scheme C leads to super-linear convergence of H_N and K_N to H_0 and K_0, respectively, for decreasing values of the mesh pitch h. We indeed observe that err_H and err_K reduce by factors greater than 2, when passing from mesh $\tilde{\Pi}_N^i$ to mesh $\tilde{\Pi}_N^{i+1}$. Differently, the approximation scheme A leads to sub-linear reduction of err_H, and marked oscillations of err_K with decreasing values of h. The approximation scheme B instead leads to non-monotonic reduction of err_H and oscillations of err_K with decreasing h. For what concerns H_N^*, we observe sub-linear reduction of e_H^* with decreasing h, and e_H^* always greater than e_H of case C for equal mesh size (cf. Table 1 and Figs. 6 and 7). The approximation K_N^* features oscillating errors e_K^* with decreasing values of h. It is worth noting that the error e_K^* is less than e_K of case C for mesh 1, and significantly greater than e_K of case C for meshes 2, 3 and 4 (cf. Table 1 and Figs. 6 and 7). We also note that the CPU time required to complete case C is markedly greater than those required to complete all the other examined approximations (cf. Table 1). This is due to the repeated calls to the external routine SURF (SURF et al., 2007) (implementing the surface fitting method given in Akima and Ortiz, 1978), which are required to perform case C. The present drawback of such an approximation scheme can be significantly mitigated by directly encoding the surface smoothing algorithm within the curvature prediction code (no calls to external routines).

5. Concluding remarks

We have presented a scale bridging approach to the curvatures of triangulated membrane networks, which allows for an accurate prediction of the bending energy of such structural models, and leads to effective polyhedral models of parametric surfaces. We have shown that the weak (oscillating) convergence of discrete curvature measures (cf. e.g., Wardetzky, 2008) can be corrected by smoothly projecting an unstructured polyhedral surface over a structured triangulation. The convergence study illustrated in Section 4 shows that such a 'regularization' approach is able to produce super-linear convergence of discrete predictions of the mean and Gaussian curvatures in the continuum limit, when sufficiently smooth projection algorithms are employed (case C). Differently, linear interpolation of unstructured polyhedral surfaces over structured meshes generates oscillating approximation errors for decreasing values of the mesh size (case B). Overall, we observe that the approximation scheme based on smooth projection operators appears rather competitive in terms of approximation accuracy, with respect to two alternative approaches frequently used in literature (Sullivan, 2008; Wardetzky, 2008), at the cost of heawier computing times. A distinctive feature of the present approach, as compared to different 'convergent' models of discrete surfaces (cf. e.g., Xu, 2004; Sullivan, 2008; Wardetzky, 2008, and therein references), consists of the use of a two-mesh technique, which converts an unstructured polyhedral surface into a structured polyhedral model.

The results of the present study pave the way to the formulation of multiscale models of membrane networks based on surface energies and coupled atomistic-continuum approaches, which can circumvent scaling limitations of fully atomistic models (Fraternali et al., 2002; Miller and Tadmor, 2009). The regularization technique formulated in Section 3 can also be employed in computational geometry problems dealing with the digital design and the prototype fabrication of freeform surfaces and vaulted structures (Bechthold, 2004; Fu et al., 2008; Pottman, 2010; Stratil, 2010; Datta et al., 2011). Additional future lines of research might regard an extensive experimentation of the proposed curvature estimation method, to be carried out in association with local maximum entropy schemes, B-Splines and/or NURBS (Cyron et al., 2009; Fraternali et al., 2012), as well as the formulation of fast implementations of the proposed regularization procedure.

Acknowledgements

F.F. is grateful to an anonymous referee for helpful comments and is thankful for support from the University of Salerno through the 2012 FARB grant 'Innovative Structures for Civil Engineering'.

References

Akima, H., Ortiz, M., 1978. Algorithm 526: bivariate interpolation and smooth surface fitting for irregularly distributed data points [E1]. ACM Trans. Math. Softw. 4, 160–176.
Bailiie, C.F., Johnston, D.A., Williams, R.D., 1990. Nonuniversality in dynamically triangulated random surfaces with extrinsic curvature. Mod. Phys. Lett. A 5, 1671–1683.
Bartesaghi, A., Sapiro, G., 2001. A system for the generation of curves on 3D brain images. Hum. Brain Mapp. 14, 1–15.
Bechthold, M., 2004. Surface structures: digital design and fabrication. ACADIA04., pp. 88–99.
Cyron, C.J., Arrojo, M., Ortiz, M., 2009. Smooth, second-order, non-negative meshfree approximants selected by maximum entropy. Int. J. Num. Methods Eng. 79, 1605–1632.
Dao, M., Li, J., Suresh, S., 2006. Molecularly based analysis of deformation of spectrin network and human erythrocyte. Mater. Sci. Eng. C 26, 1232–1244.
Datta, S., Sharman, M., Hanafin, S., Chang, T.-W, 2011. Computation and construction of vault geometry prototypes. In: Proceedings of the 28th International Symposium on Automation and Robotics in Construction, ISARC 2011, pp. 113–117.
Davini, C., Paroni, R., 2003. Generalized hessian and external approximations in variational problems of second order. J. Elast. 70, 149–174.
Discher, D.E., Boal, D.H., Boey, S.K., 1997. Phase transitions and anisotropic responses of planar triangular nets under large deformation. Phys. Rev. E 55 (4), 4762–4772.
El Sayed, T., Mock, W., Mota, A., Fraternali, F., Ortiz, M., 2009. Computational assessment of ballistic impact on a high strength structural steel/polyurea composite plate. Comput. Mech. 43 (4), 525–534.
Espriu, D., 1987. Triangulated random surfaces. Phys. Lett. B 194, 271–276.
Fraternali, F., 2007. Error estimates for a lumped stress method for plane elastic problems. Mech. Adv. Mater. Struct. 14 (4), 309–320.
Fraternali, F., Angelillo, M., Fortunato, A., 2002. A lumped stress method for plane elastic problems and the discrete-continuum approximation. Int. J. Solids Struct. 39, 6211–6240.
Fraternali, F., 2010. A thrust network approach to the equilibrium problem of unreinforced masonry vaults via polyhedral stress functions. Mech. Res. Commun. 37, 198–204.
Fraternali, F., Lorenz, C., Marcelli, G., 2012. On the estimation of the curvatures and bending rigidity of membrane networks via a local maximum-entropy approach. J. Comput. Phys. 231, 528–540.

Fraternali, F., Marcelli, G., 2012. A multiscale approach to the elastic moduli of biomembrane networks. Biomech. Model. Mech. 11, 1097–1108.
Fu, J., Joshi, S.B., Simpson, T.W., 2008. Shape differentiation of freeform surfaces using a similarity measure based on an integral of Gaussian curvature. CAD Comput. Aided Des. 40 (3), 311–323.
Gompper, G., Kroll, D.M., 1996. Random surface discretization and the renormalization of the bending rigidity. J. Phys. I – France 6, 1305–1320.
Hartmann, D., 2010. A multiscale model for red blood cell mechanics. Biomech. Model. Mechanobiol. 9, 1–17.
Helfrich, W., 1973. Elastic properties of lipid bilayers: theory and possible experiments. Z. Naturforschung C 28, 693–703.
Helfrich, W., Kozlov, M.M., 1993. Bending tensions and the bending rigidity of fluid membranes. J. Phys. II – France 3, 287–292.
Kühnel, W., 2002. Differential Geometry. Curves – Surfaces – Manifolds. American Mathematical Society, Providence, RI.
Marcelli, G., Parker, H.K., Winlove, P., 2005. Thermal fluctuations of red blood cell membrane via a constant-area particle-dynamics model. Biophys. J. 89, 2473–2480.
Miller, R.E., Tadmor, E.B., 2009. A unified framework and performance benchmark of fourteen multiscale atomistic/continuum coupling methods. J. Model. Simul. Mater. Sci. 17, 053001.
Pottman, H., 2010. Architectural geometry as design knowledge. Architect. Des. 80 (4), 72–77.
Pottman, H., Asperl, A., Kilian, A., 2007. Architectural Geometry. Bentley Institute Press, Exton.
Raney, J.R., Fraternali, F., Amendola, A., Daraio, C., 2011. Modeling and in situ identification of material parameters for layered structures based on carbon nanotube arrays. Compos. Struct. 93 (11), 3013–3018.
Rypl, D., Bittnar, Z., 2006. Generation of computational surface meshes of STL models. J. Comput. Appl. Math. 192 (1), 148–151.
Schmidt, B., Fraternali, F., 2012. Universal formulae for the limiting elastic energy of membrane networks. J. Mech. Phys. Solids 60, 172–180.
Seung, H.S., Nelson, D.R., 1988. Defects in flexible membranes with crystalline order. Phys. Rev. A 38, 1005–1018.
Stratil, J., 2010. Evolutionary formfinding – conception of effective structures by means of interactive patterns. In: Structures and Architecture – Proceedings of the 1st International Conference on Structures and Architecture, ICSA 2010, pp. 707–714.
Sullivan, J.M., 2008. Curvatures of smooth and discrete surfaces. In: Bobenko, A.I., Schröder, P., Sullivan, J.M., Ziegler, G.M. (Eds.), In: Discrete Differential Geometry, vol. 38. Oberwolfach Seminars, Birkhaeuser Verlag Basel, Switzerland, pp. 175–188.
SURF, Visual Numerics, Inc., 2007. Smooth bivariate interpolant to scattered data that is locally a quintic polynomial in two variables. IMSL® Fortran Numerical Math Library. http://www.vni.com
Taubin, G.,1995. Estimating the tensor of curvature of a surface from a polyhedral approximation. In: Proceedings of the 5th International Conference on Computer Vision (ICCV'95). MIT, Cambridge, MA, pp. 902–907.
Wardetzky, M., 2008. Convergence of the cotangent formula: an overview. In: Bobenko, A.I., Schröder, P., Sullivan, J.M., Ziegler, G.M. (Eds.), In: Discrete Differential Geometry, 38. Oberwolfach Seminars, Birkhaeuser Verlag Basel, Switzerland, pp. 275–286.
Xu, G., 2004. Convergent discrete Laplace-Beltrami operators over triangular surfaces. Geom. Model. Process., 195–204.